Journal of Thermal Analysis and Calorimetry (2021) 146:493–507
https://doi.org/10.1007/s10973-020-10022-4

Experimental investigation of rheological properties and thermal conductivity of SiO_2–P25 TiO_2 hybrid nanofluids

Thong Le Ba[1] · Zalán István Várady[1] · István Endre Lukács[2] · János Molnár[3] · Ida Anna Balczár[4] · Somchai Wongwises[5,6] · Imre Miklós Szilágyi[1]

Received: 19 May 2020 / Accepted: 2 July 2020 / Published online: 21 July 2020

Abstract

Over many years, great efforts have been made to develop new fluids for heat transfer applications. In this paper, the thermal conductivity (TC) and viscosity of SiO_2–P25 TiO_2 (SiO_2–P25) hybrid nanofluids were investigated for different nanoparticle volume concentrations (0.5, 1.0 and 1.5 vol%) at five various temperatures (20, 30, 40, 50 and 60 °C). The mixture ratio (SiO_2:P25) in all prepared hybrid nanofluids was 1:1. Besides, pure SiO_2, P25 nanofluids were prepared with the same concentrations for comparison with the hybrid nanofluids. The base fluid used for the preparation of nanofluids was a mixture of deionized water and ethylene glycol at a ratio of 5:1. Before preparing the nanofluids, the nanoparticles were analyzed with energy-dispersive X-ray analysis, scanning electron microscope, X-ray powder diffraction, and Fourier transform infrared spectroscopy. The zeta potentials of the prepared nanofluids except SiO_2 nanofluids were above 30 mV. These nanofluids were visually observed for stability in many days. The TC enhancement of the hybrid nanofluid was higher than the pure nanofluid. In particular, with 1.0 vol% concentration, the maximum enhancement of SiO_2, P25 and SiO_2–P25 nanofluids were 7.5%, 9.9% and 10.5%, respectively. The rheology of the nanofluids was Newtonian. The viscosity increment of SiO_2, P25 and hybrid nanofluids were 19%, 32% and 24% with 0.5 vol% concentration. A new correlation was developed for the TC and dynamic viscosity of SiO_2–P25 hybrid nanofluid.

Keywords Silicon dioxide · Titanium dioxide · Base fluid · Nanofluids · Thermal conductivity · Viscosity

Introduction

Masuda et al. [1] and Choi [2] started working with nanofluids as an effective heat transfer fluid. In recent years, the nanofluids have become more popular due to the improvement of their thermal characteristics compared to conventional fluids like EG, water and oil. There are a lot of engineering applications of nanofluids such as solar

✉ Thong Le Ba
kenty9x@gmail.com

Zalán István Várady
varadyzalan@gmail.com

István Endre Lukács
lukacs.istvan@energia.mta.hu

János Molnár
molnar.janos@mail.bme.hu

Ida Anna Balczár
balczari@almos.uni-pannon.hu

Somchai Wongwises
somchai.won@kmutt.ac.th

Imre Miklós Szilágyi
imre.szilagyi@mail.bme.hu

1 Department of Inorganic and Analytical Chemistry, Budapest University of Technology and Economics, Muegyetem rakpart 3., Budapest 1111, Hungary

2 Centre for Energy Research, Institute for Technical Physics and Materials Science, Hungarian Academy of Sciences, Konkoly Thege M. út 29-33, Budapest 1121, Hungary

3 Department of Physical Chemistry and Materials Science, Budapest University of Technology and Economics, Muegyetem rakpart 3., Budapest 1111, Hungary

4 Institute of Materials Engineering, Faculty of Engineering, University of Pannonia, Egyetem út 10, Veszprém 8200, Hungary

5 Department of Mechanical Engineering, Faculty of Engineering, King Mongkut's University of Technology Thonburi, Bangmod, Bangkok 10140, Thailand

6 National Science and Technology Development Agency (NSTDA), Khlong Luang, Pathum Thani 12120, Thailand

thermal, automobile and electronic cooling applications [3–8]. It is evidenced that the TC of nanofluids mostly depends on the property of nanoparticles [9].

Compared to the standard nanofluid, hybrid nanofluids (HNs) offer even more possibilities. The composite nanofluids or HNs are the colloidal dispersion of two or more kinds of nanoparticles with the BF [10]. According to Sundar et al. [11], there are three main types of HN: metal matrix, ceramic matrix and polymer matrix nanocomposites. The nanoparticles can be prepared by various techniques or by the combination of different techniques such as ball milling, chemical vapor deposition and plasma treatment [12–16]. There are two types of nanofluid preparations, including a one-step method and a two-step method. In the first one, the production of nanoparticles and dispersion of nanoparticles into BF are combined in one step. In the two-step method, the nanoparticles are prepared first and then dispersed into the BFs [17]. Because of new characteristics, HNs have been investigated with different nanoparticles, BFs, temperatures and concentrations. Nabil et al. [18] and Ganvir et al. [19] presented some reviews about their thermophysical properties. Hybrid nanofluid with carbon nanotubes grafted to alumina/iron oxide spheres dispersed in poly-alpha-olefin was studied by Han et al. [20]. A TC enhancement of 21% for a volume concentration of 0.2% was obtained. The carbon nanotubes play an important role in the augmentation of TC. The Al_2O_3–Cu/water HNs with volume concentrations from 0.1 to 2% were investigated by Suresh et al. [21]. A maximum TC enhancement of 12.11% compared to single Al_2O_3 was shown at a volume concentration of 2%. Madhesd et al. [22] investigated Cu-TiO_2 HNs in the application of water-based coolant. The TC of the fluid increased by 48.4% compared to the BF of water up to 0.7 vol% of the hybrid nanocomposite. It was found that the functionalized surface and the high crystallinity of the nanocomposite improved the enhancement of TC. In recent years, further investigations on the viscosity of HNs have been performed [23–26]. A numerical study on hybrid nanocomposite of TiO_2, Al_2O_3 and SiO_2 nanoparticles dispersed in water was performed [27]. Al_2O_3 (25%) was mixed with TiO_2 (75%) or SiO_2 (75%) for preparing HNs at concentrations of 0.5, 1.0 and 1.5 vol%. An experimental investigation on the rheological behavior of Fe–CuO HNs was performed in water–EG at a proportion of 20:80 vol%. The concentration range of HNs was 0.04–1.5 vol%. They found that at low concentration, the rheology of HNs was Newtonian, whereas at high concentration, HN exhibited non-Newtonian behavior (shear-thinning) [28]. Sundar et al. and Zakaria et al. [29, 30] investigated the TC of nanofluids with the BF of DW and EG mixture. They found that the enhancement of TC was affected by volume concentration and temperature. Additionally, the particle size and stability of nanofluid contributed to the improvement of TC [31, 32]. It was found that the combination of nanofluids has higher TC and lower dynamic viscosity [33–35].

From the results of Agresti et al. [36] and Turgut et al. [37], the TC of pure TiO_2 nanofluid was higher than of pure SiO_2 nanofluid; meanwhile, the viscosity of SiO_2 nanofluid was lower than of TiO_2 nanofluid. Producing hybrid or composite nanofluids from SiO_2 and TiO_2 nanoparticles is expected to enhance the useful characteristic of single nanofluids, such as higher TC of TiO_2 nanofluid and lower viscosity of SiO_2 nanofluid. Some works have been performed to evaluate the TC of SiO_2–TiO_2 HNs. Nabil et al. used TiO_2 (50 nm) and SiO_2 (22 nm) nanoparticles for investigating the heat transfer enhancement of HNs with different concentrations (0.5–3 vol%), temperatures (30–80 °C), BF ratios, nanoparticle ratios and forced convection mode [35, 38–40]. They found that the TC enhancement of HNs was 22.1% at 3.0 vol% and 70 °C compared to the BF. Meanwhile, 62.5% increment of relative viscosity was observed for 3.0% volume concentration.

Due to the instability in nanofluids, the aggregation of nanoparticles causes a decrease in the thermo-physical characteristics. This is a critical problem for nanofluids, which limits their engineering applications. The preparation of nanofluids with good stability is the priority challenge [41, 42]. Nanoparticles cause the TC and viscosity of nanofluids to be higher due to the motion of nanoparticles in suspension. The instability of nanofluids and higher viscosity result in decreasing the heat transfer. Therefore, the stability, viscosity and TC should be investigated in detail [17]. Besides, the results obtained in different research groups are not consistent. Also, studying the properties of the nanofluids is often not completely performed. The theoretical understanding of the mechanisms is the lack of improvement of properties [43].

To the best of authors' knowledge, there are no reports on the TC enhancement and viscosity of these SiO_2–P25 HNs. The purpose of this research is to prepare the stable SiO_2–P25 HNs with SiO_2 (10–20 nm) and P25 (21 nm) nanoparticles and investigate their rheological property and TC. The experimental study is conducted for 0.5, 1.0 and 1.5% volume concentrations with the nanoparticle mixture ratio (SiO_2:P25) of 1:1. The temperatures during the experiments are from 20 to 60 °C. The properties of the nanoparticles are investigated with EDX, SEM, XRD and FT-IR. Lastly, the relevant correlations are proposed using the results of the present study.

Materials and methods

Materials

Silicon dioxide (SiO_2) nanopowder (99.5%, 10–20 nm, 637238-50G), P25 titanium dioxide (P25) nanopowder (≥ 99.5%, 21 nm, 718467-100G) and ethylene glycol (≥ 99%, 102466-1L) were purchased from Sigma-Aldrich, Hungary. The materials were analytical reagent grades and utilized as original, with no other change. DI and EG were used as BFs. DI was produced in the Department of Inorganic and Analytical Chemistry laboratory, Budapest University of Technology and Economics (Hungary). Tables 1 and 2 show the properties of P25, SiO_2 nanoparticles, ethylene glycol and water.

Preparation of nanofluid

SiO_2, P25 nanofluids and SiO_2–P25 HNs were prepared by dispersing different amounts of SiO_2, P25 nanoparticles and SiO_2–P25 mixture (1:1 volume ratio) in DI and EG mixture (5:1). SiO_2–P25 in amounts of 0.5 vol%, 1.0 vol% and 1.5 vol% was dispersed in an appropriate mass of DI and EG. Then, SiO_2–P25 HN colloidal solutions were sonicated at 130 W and 45 kHz using an ultrasonication instrument for 1 h. Table 3 shows pure SiO_2, P25 nanofluids and SiO_2–P25 HN sample specifications.

Characterization methods

The crystal structure of SiO_2 and P25 was investigated by using PANalytical X'PERT PRO MPD XRD with Cu K_α irradiation. Data were collected for the 2θ range of 5° to 65° at a resolution of 3 degrees/min. Morphological characterization of SiO_2 and P25 was done by LEO 1440 XB SEM at 5 kV in a high vacuum mode with a secondary electron detector. The chemical composition of SiO_2 and P25 was studied by using EDX analysis with JEOL JSM-5500LV electron microscope. Infrared spectra of nanopowders were studied by Excalibur FTS 3000 Bio-Rad FT-IR in the 400–4000 cm^{-1} domain in transmittance mode, the sensitivity of measurements was 4 cm^{-1}, and the number of scans was 64.

A Brookhaven ZETAPALS device was used for ZP measurement of SiO_2–P25 HNs. The ZP (ζ) was obtained from electrophoretic mobility (EM) of particles thanks to the Henry equation by applying the Smoluchowski approximation [46]. Each sample was tested three times, and the average value was reported.

The rheological behavior of SiO_2–P25 HN was measured using a rotation viscometer (Anton Paar Physica MCR 301) at different shear rates and temperatures. The number of data points per measurement was 15. The amplitude was 5%, and the angular frequencies were between 0.6 and 3600 s^{-1}.

The TC of SiO_2–P25 HN samples was measured based on the modified transient plane source technique using a TCi Thermal conductivity analyzer. The TC of all samples was measured at five different temperatures of 20, 30, 40, 50 and 60 °C. A temperature-controlled oven was used to maintain the temperature at the desired set point. All samples were kept in the oven for 30 min to reach that temperature. Three TC measurements were taken for each sample, and an average value was reported.

Table 1 Properties of P25 and SiO_2 nanoparticles [44]

Properties	SiO_2	P25
Color	White	White
Molecular mass/g mol^{-1}	60.08	79.87
Average particle diameter/nm	10–20	21
Density/kg m^{-3}	2220	4260
Melting point/°C	2230	1850

Table 2 Properties of ethylene glycol and water [45]

Properties	Ethylene glycol	Water
Formula	$C_2H_6O_2$	H_2O
Molecular mass/g mol^{-1}	62.07	18.02
Freezing point/°C	− 12.7	0
Boiling point, at 101.3 kPa/°C	198	100
Viscosity at 20 °C/mPas	20.9	1
Density/kg m^{-3}	1113	997
Thermal conductivity/W mK^{-1}	0.258	0.609
Specific heat at 20 °C/J kg^{-1} K^{-1}	2347	4186

Table 3 Specification of SiO_2, P25 nanofluids and SiO_2–P25 hybrid nanofluid samples

Sample names	SiO_2/vol%	P25/vol%	DI and EG mixture (5:1)/vol%
SiO_2-0.5	0.50	0.00	99.50
SiO_2-1.0	1.00	0.00	99.00
SiO_2-1.5	1.50	0.00	98.50
P25-0.5	0.00	0.50	99.50
P25-1.0	0.00	1.00	99.00
P25-1.5	0.00	1.50	98.50
SiO_2–P25-0.5	0.25	0.25	99.50
SiO_2–P25-1.0	0.50	0.50	99.00
SiO_2–P25-1.5	0.75	0.75	98.50

Results and discussion

SiO_2 and P25 structure

Figure 1 shows the XRD pattern of SiO_2 and P25. For the XRD pattern of SiO_2 (Fig. 1a), the amorphous nature of the used nano-SiO_2 could be seen from the diffractogram [47]. The broad diffraction peak confirmed a completely amorphous structure. Except for a broad band centered at $2\theta = 22.5°$, there is no diffraction peak observed. This peak is the characteristic peak for amorphous SiO_2. It also reveals no impurity peaks for SiO_2 nanoparticles. Based on the XRD patterns of P25 (Fig. 1b), P25 consists of rutile and anatase phases. The anatase form is the main component with peaks at 2θ values of 25.4°, 37.9°, 48.1°, 54°, 55.1° and 62.8°. The rutile phase is an adjunct at 2θ values of 27.6°, 36.2°, 41.4° and 54.4° [48]. There are not any lines corresponding to any impurity phases, so the high purity of the P25 sample is indicated.

Figure 2 shows the SEM image of the morphological structure of nano-SiO_2. It can be observed from the SEM image that nano-SiO_2 has a nanosize of ca. 15 nm in accordance with the manufacturer's specifications. The SEM image of nano-P25 is shown in Fig. 3. It can be found that the particle size is 10–20 nm. The P25 and SiO_2 nanoparticles tend to stick together into the larger particles. The aggregation size of SiO_2 is larger than of P25.

The functional groups support the achievement of a proper dispersion. The FT-IR spectrum of P25 nanoparticles is shown in Fig. 4. The broadband centered at around 600 cm^{-1} is assigned to the bending vibration (Ti–O-Ti) bonds in the TiO_2 lattice. The broadband centered at around 3420 cm^{-1} is attributed to the intermolecular interaction of the hydroxyl group (–OH) with H_2O molecule on TiO_2

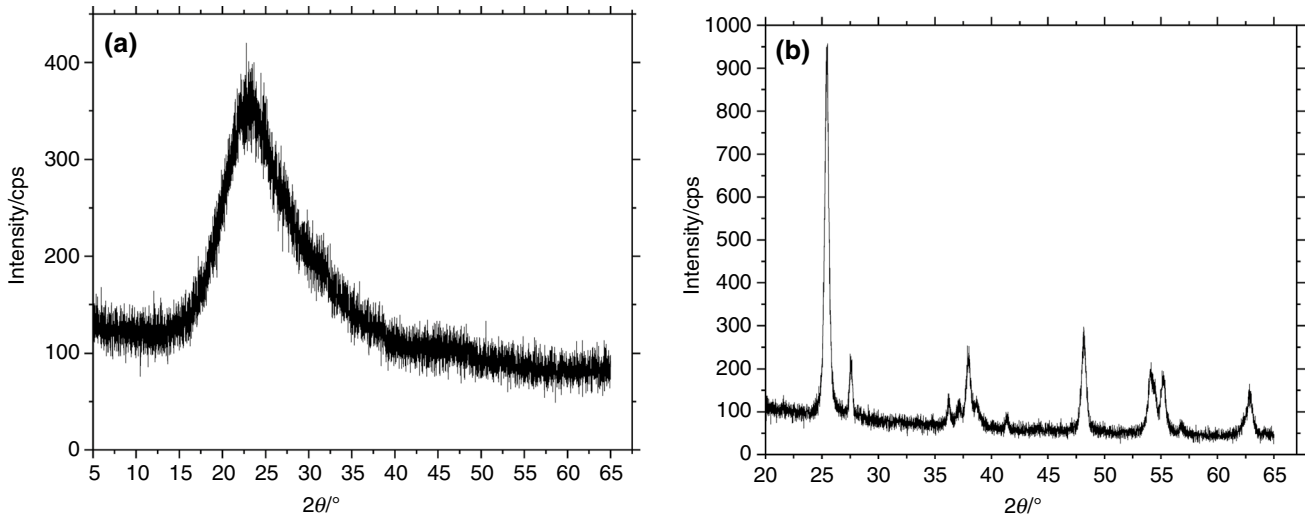

Fig. 1 XRD pattern of SiO_2 (**a**), P25 (**b**) at the following XRD circumstances: X-ray: 40 kV, 30 mA. Scan speed: 3.0° min^{-1}

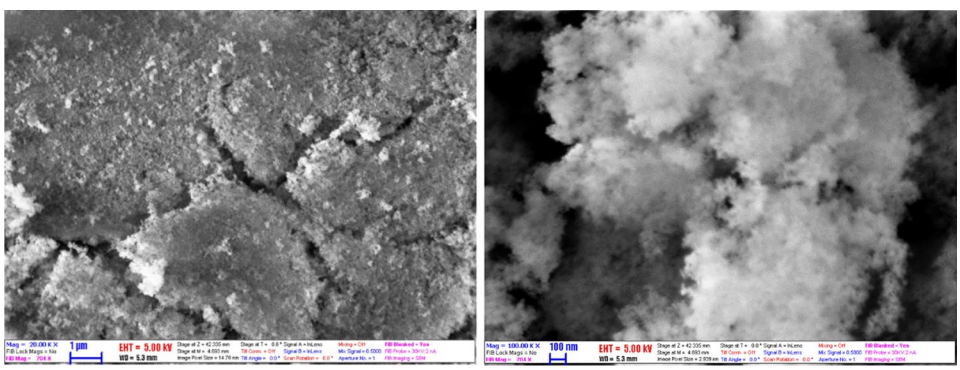

Fig. 2 SEM images of SiO_2 nanoparticles

surface. The peak at around 1650 cm^{-1} confirms the typical bending vibration of –OH group [49]. Figure 5 shows the FT-IR spectrum of SiO_2 nanoparticles. The peaks at around 3420 cm^{-1} and 1630 cm^{-1} can be ascribed to the –OH stretching and bending vibrations of absorbed water molecules on the SiO_2 nanoparticles, respectively. The peaks at 1101 and 475 cm^{-1} refer to the Si–O-Si asymmetric stretching and bending vibrations. The Si–O bond stretching vibration appears at 1384 cm^{-1}. The peaks at 961 cm^{-1} and 801 cm^{-1} are attributed to the Si–O-(H-H_2O) bending vibrations and in-plane bending vibrations of geminol groups, respectively.

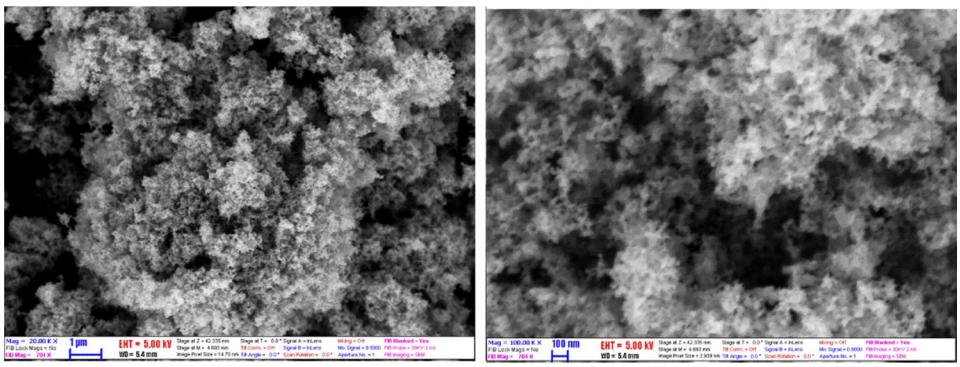

Fig. 3 SEM images of P25 nanoparticles

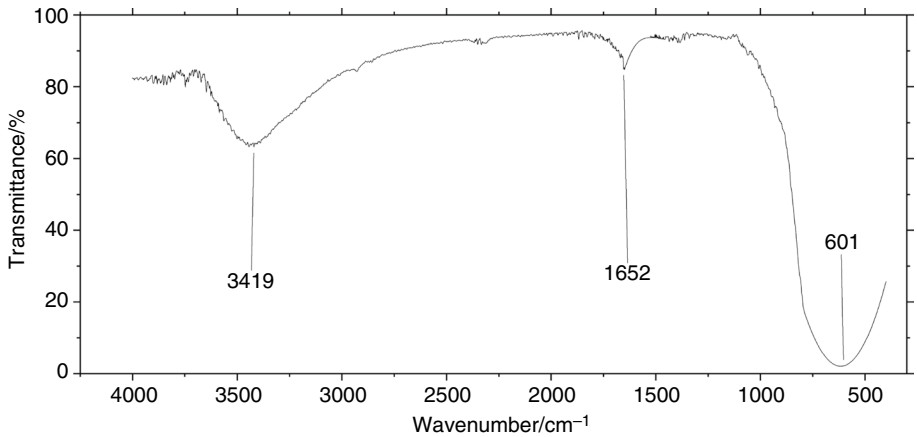

Fig. 4 FT-IR spectrum of P25 nanoparticles

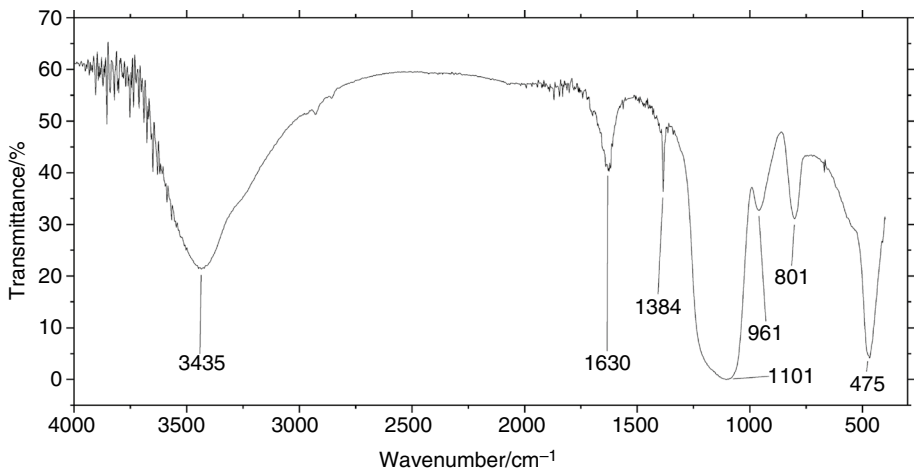

Fig. 5 FT-IR spectrum of SiO_2 nanoparticles

Table 4 EDX results of P25 and SiO_2 nanoparticles

SiO_2/atom%		P25/atom%	
Si	O	Ti	O
33.68	66.32	30.57	69.43

Table 5 ZP of 0.5 vol% SiO_2–P25 nanofluids with different surfactants

Surfactant	ZP of 0.5 vol% SiO_2–P25 hybrid nanofluid/mV
N/A	− 30.42
CTAB	− 19.09
SDBS	− 10.46
SCMC	− 10.09
TX	− 17.34

Table 4 contains the EDX results of P25 and SiO_2 nanoparticles. The results are the average values of different measurement points in the atomic percentage. These results confirm the chemical composition of the used nanoparticles.

Zeta potential measurement

Table 5 shows the ZP of 0.5 vol% SiO_2–P25 HN with different surfactants. For improving the stability of SiO_2–P25 HN, different surfactants are used such as CTAB (cetyl trimethylammonium bromide), SDBS (sodium dodecylbenzenesulfonate), SCMC (sodium carboxymethylcellulose) and TX (Triton X-100). Among the used surfactants, the CTAB gives the best result with − 19.09 mV. According to the ZP values, the SiO_2–P25 HNs have the best stability without any surfactants. However, by visual observation, it can be seen that the role of surfactant is not much important in improving the stability of the HNs. Further studies can focus on the stability of nanofluid by changing surfactant concentration, other types of surfactants and solvents.

Colloidal solutions with ZP s lower − 30 mV have acceptable stability [50, 51]. Table 6 shows ZP values of SiO_2, P25 pure nanofluids and SiO_2–P25 hybrid nanofluids with different concentrations. The ZP of 0.5, 1.0 and 1.5 vol% SiO_2–P25 HN was − 30.42 mV, − 33.03 mV and − 43.33 mV, respectively. This shows the stability of nanofluids. These ZP values indicate the slower aggregation behavior of SiO_2–P25 nanoparticles by increasing the concentration. It means that by increasing the concentrations of nanofluids, the negative electrical surface charge of SiO_2–P25 increased; thus, the -OH groups were ionized. P25 nanofluids provide good stability with high ZP. ZP results showed that SiO_2 nanofluids have moderate stability. By visual observation, it is confirmed that these nanofluids are stable for several days.

Table 6 ZP of SiO_2, P25 nanofluids and SiO_2–P25 hybrid nanofluids with different concentrations

Nanofluids	Zeta potential/mV
SiO_2–P25-0.5	− 30.42
SiO_2–P25-1.0	− 33.03
SiO_2–P25-1.5	− 43.33
SiO_2-0.5	− 23.04
SiO_2-1.0	− 24.17
SiO_2-1.5	− 25.23
P25-0.5	34.49
P25-1.0	33.28
P25-1.5	30.94

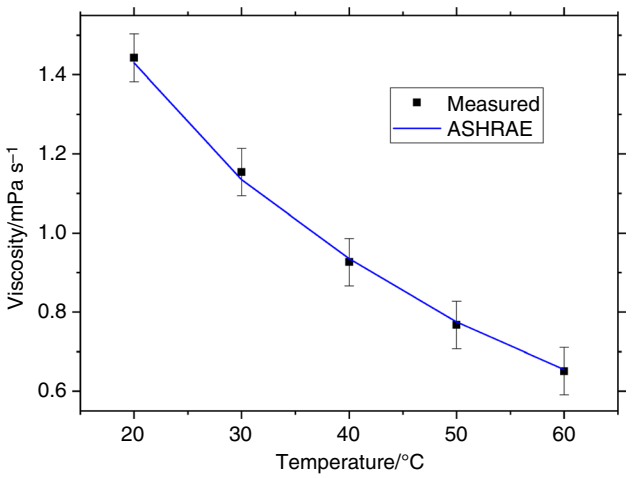

Fig. 6 Comparison between the measured viscosity of DI/EG base fluid and ASHRAE results [45]

Rheological properties of SiO_2–P25 hybrid nanofluid

The viscosity of the BF was measured, and the results are compared to the literature in order to verify the measurement. The results are compared to the BF in the ASHRAE standard [45] as shown in Fig. 6. The maximum error is less than 1.0%, and the measurements are trustable.

For determining the rheological behaviors of SiO_2–P25 HNs, the shear stress at different shear rates is investigated for three volume concentrations of 0.5, 1.0 and 1.5 at five temperatures: 20, 30, 40, 50 and 60 °C as shown in Fig. 7. Shear stress of all SiO_2–P25 HN samples decreases with increasing temperature and increases with increasing fraction of nanofluids.

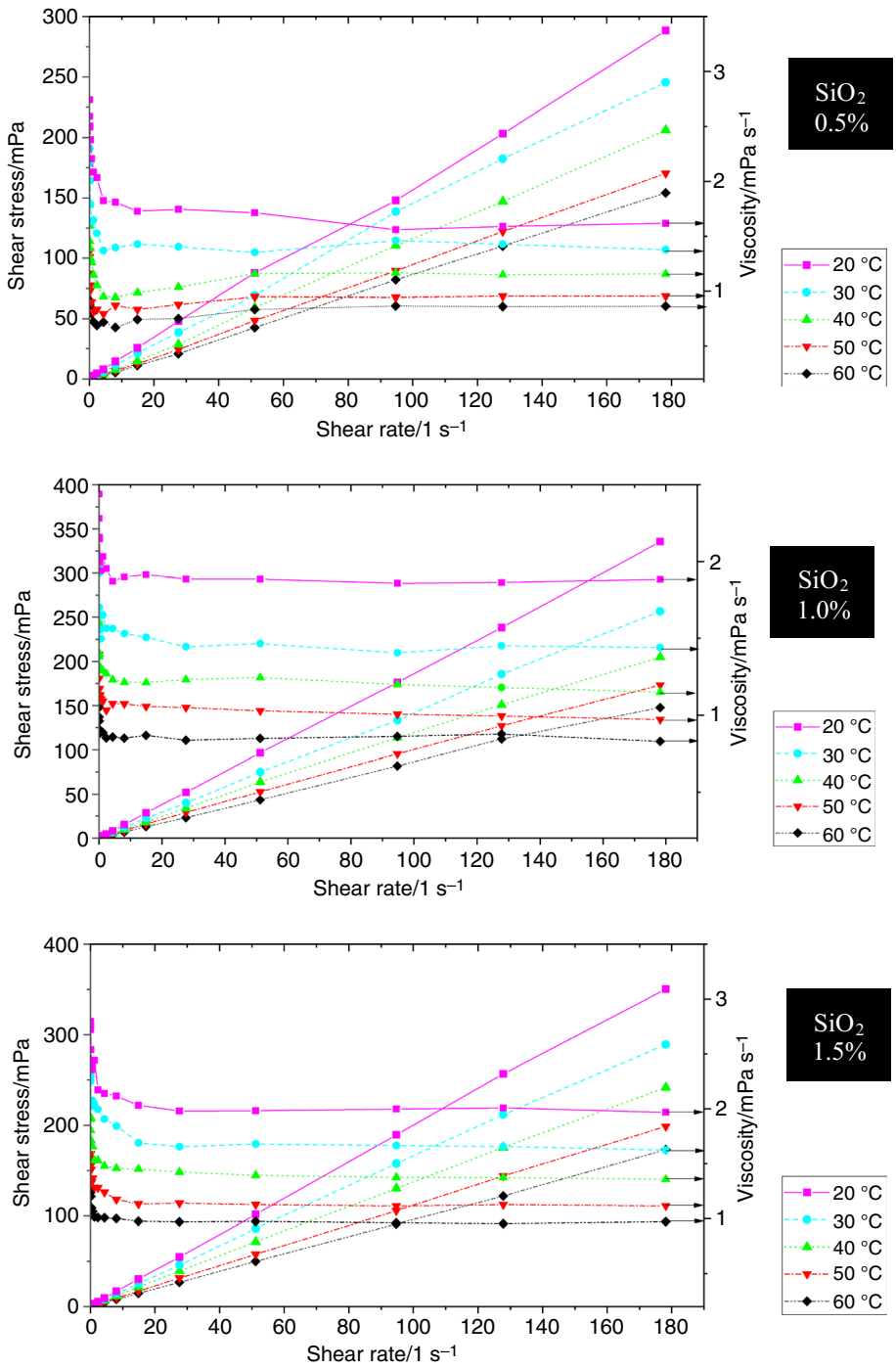

Fig. 7 Shear stress–shear rates diagram

This reduction behavior of viscosity may be caused because higher temperature increases the Brownian and thermal motion of molecules and their average velocity, leading to weakened intermolecular interaction and adhesion forces between molecules [25, 52]. For low shear rates (less than 5 s^{-1}), the nanofluid behaves as a non-Newtonian fluid or shear-thinning fluid. It means the viscosity of all HNs decreases with the increase in the shear rate. In a case of high shear rates, the viscosity of SiO_2–P25 HNs is almost independent of the applied shear rate. This means the HN is Newtonian as shown in Fig. 7. Bahrami et al. [28] and Nabil et al. [38] found the Fe–CuO nanofluids and TiO_2-SiO_2 nanofluids owned Newtonian rheological behavior for different temperatures and concentrations. These results indicate that the properties of nanoparticles and temperature are important factors in the rheological properties of nanofluids. The rheological behavior generally depends on particle size and morphology, nanoparticle fraction, BF, electro-viscous

Fig. 7 (continued)

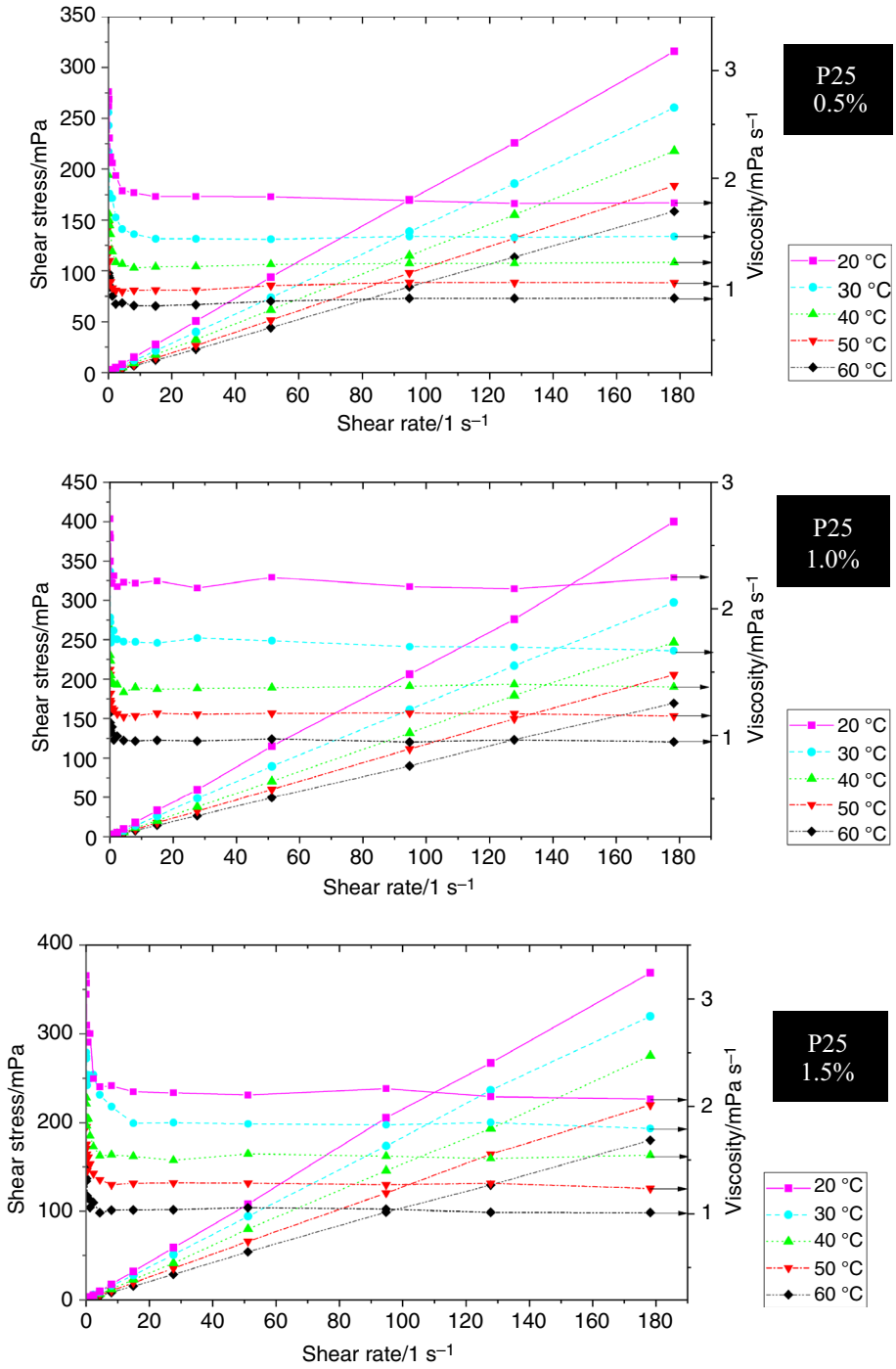

effects and solution chemistry-related surface layer [53]. Mehrali et al. showed that at low shear rates, the structure of fluid changes temporarily when the spindle rotates in the fluid, and molecules are gradually arranged in the direction of increasing shear, causing less reduction in viscosity. Nevertheless, the maximum amount of possible shear ordering was attained as the shear rate was high enough. The larger aggregate molecules were broken down into smaller sizes, causing less viscosity [54]. With the presence of

Fig. 7 (continued)

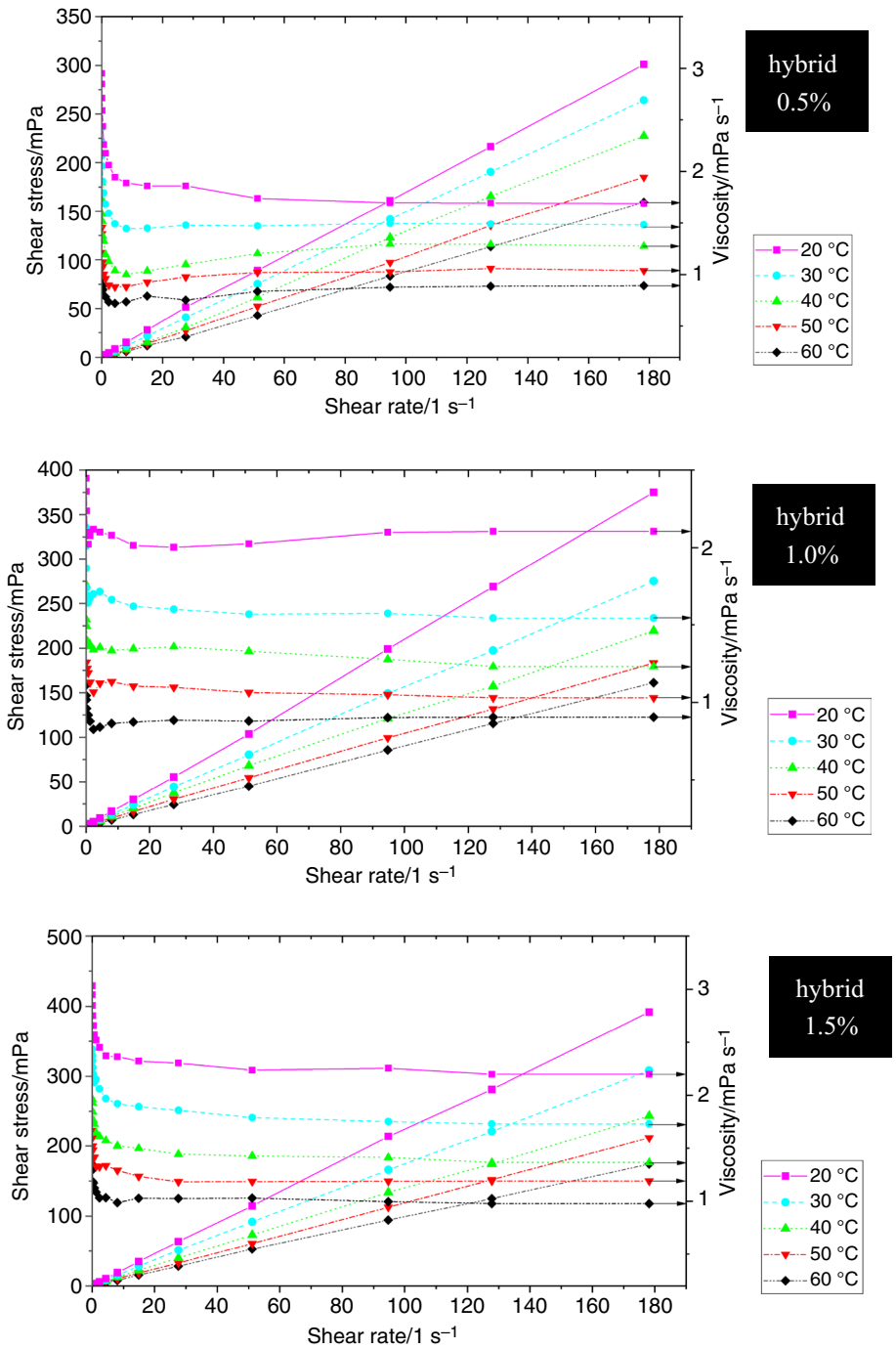

nanoparticles in HNs, it can be explained that the viscosity of SiO_2–P25 HNs is higher than the BF.

Figure 8 shows the relative viscosity of SiO_2–P25 HNs. The relative viscosity increases with the increase in the volume concentration, while temperature does not play an important role. The lowest relative viscosity of 24% increase was obtained for 0.5% volume fraction, while the highest enhancement of relative viscosity was 58% for 1.5 vol%. The relative viscosity increased from 24 to 58% compared to the BF.

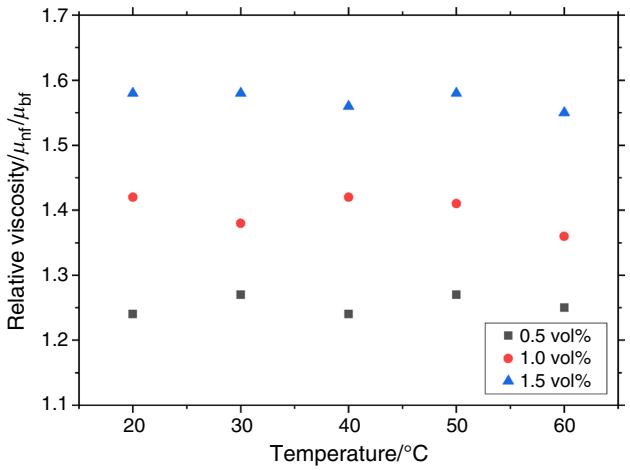

Fig. 8 Relative viscosity of SiO_2–P25 HNs at different temperatures

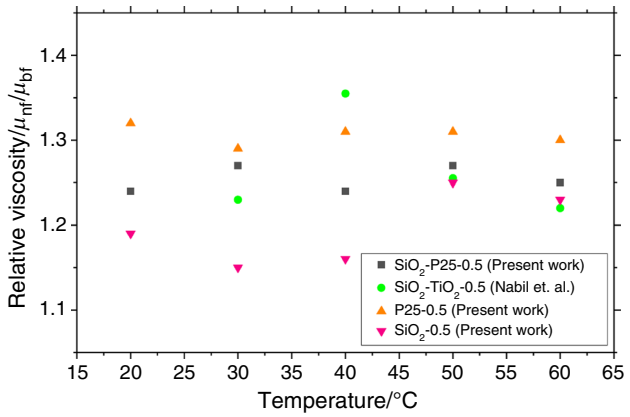

Fig. 9 Comparison of the relative viscosity between the present work and the result of Nabil et al. [38]

Figure 9 shows a comparison of the relative viscosity between the present work (0.5 vol%) with the data from Nabil et al. [38]. The results from the present research show little higher relative viscosity than the literature between 20 and 60 °C. The SiO_2 nanofluids still have the smallest relative viscosity, while the P25 nanofluids have the highest viscosity. The viscosity strongly depends on nanoparticles, BFs and concentrations.

Thermal conductivity of SiO_2–P25 hybrid nanofluid

The TC of all SiO_2–P25 HNs at various temperatures is shown in Fig. 10. The calibration tests for distilled water are verified before the measurement of samples, and the results are obtained within 0.5% error. All SiO_2–P25 HNs show higher TC compared to DI/EG mixture at all temperatures. SiO_2–P25 HNs at 0.5 vol%, 1.0 vol% and 1.5 vol% showed 4.72%, 7.19% and 9.03% TC enhancement compared to the EG/DI mixture at 20 °C, respectively. The TC of SiO_2–P25 HNs is enhanced by increasing the temperature. Nevertheless, the effect of temperature and concentration on the enhancement of TC is different. On the one hand, the temperature causes the TC of nanofluids to be higher because of the reduction in viscosity and the augmentation in Brownian motion of nanoparticles [55]. On the other hand, the relationship between TC enhancement and concentration of SiO_2–P25 nanoparticles is not completely linear. This is understandable; as the number of nanoparticles in the solution increases, the TC of the solution also increases. In addition to the concentration and temperature, the extent of TC enhancement of nanofluids depends on the type of used nanomaterials, pH, surfactants and the type of BF, which influence the motion of particles in suspension.

Figure 11 shows the enhancement of TC obtained from the present work and previous studies. It can be seen that the TC of the HNs in the present research is higher than the TC of SiO_2 pure nanofluid, P25 nanofluid and even SiO_2–P25 HNs. This can be explained that P25 contributes greatly to increasing the TC of the HNs.

Regression correlations

The following correlation is proposed based on experimental data:

$$\text{Relative viscosity} = \frac{\mu_{nf}}{\mu_{bf}} = 1.1036\left(1+\frac{T}{70}\right)^{0.03667}\left(1+\frac{\phi}{100}\right)^{22.4472}, \quad (1)$$

where μ_{nf} and μ_{bf} represent the viscosity of nanofluid and viscosity of BF, while φ and T are volume concentration and temperature. This correlation is valid for a range of concentrations $0 \le \boldsymbol{\Phi} \le 1.5\%$ and range of temperatures $30\,°C \le T \le 70\,°C$. The average and standard deviations are 1.1% and 1.2%. The maximum deviation is found to be 2.4%. Figure 12 shows the tabulation of viscosity from the experiment and Eq. 1.

Meanwhile, Eq. 2 is proposed based on experimental data where k_{nf} and k_{bf} represent the TC of nanofluid and TC of BF.

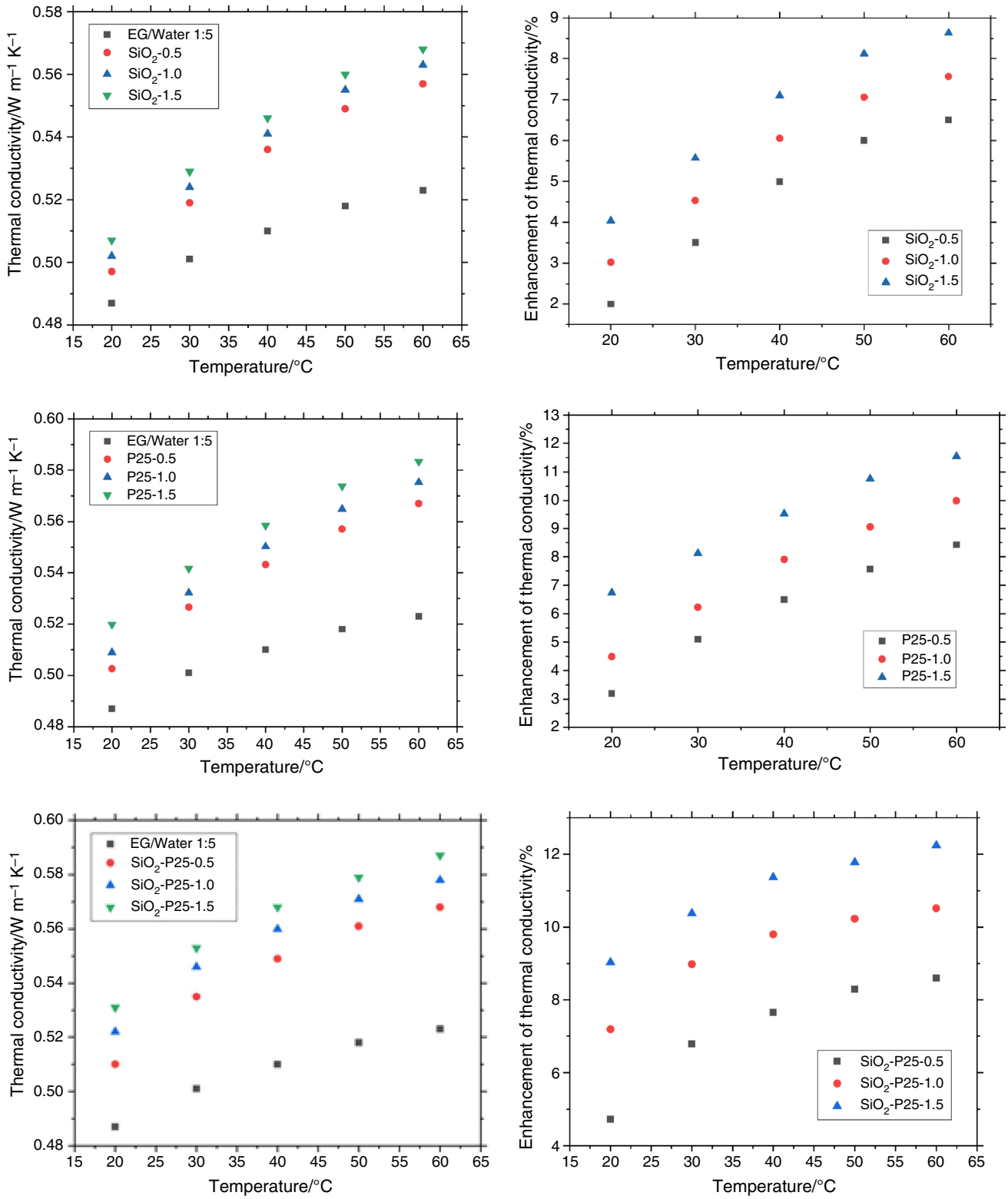

Fig. 10 TC and enhancement of TC of pure SiO_2, P25 and SiO_2–P25 hybrid nanofluids at different temperatures

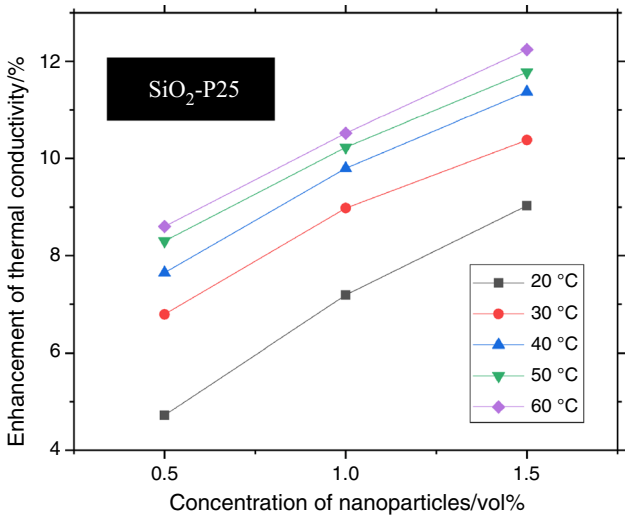

Fig. 10 (continued)

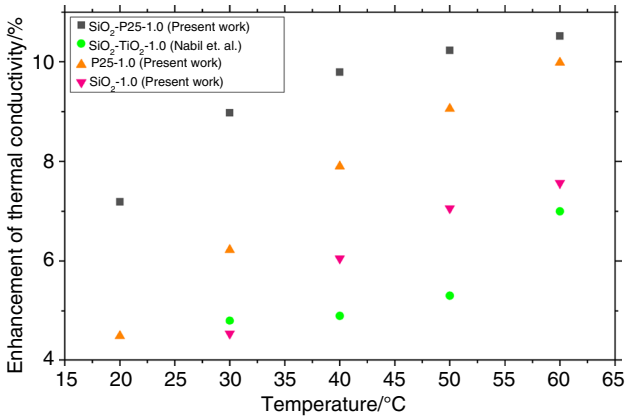

Fig. 11 Comparison of the enhancement of TC between the present work and the result of Nabil et al. [38]

$$k_{\mathrm{nf}} = k_{\mathrm{bf}} * 1.0156\left(1+\frac{T}{70}\right)^{0.0848}\left(1+\frac{\phi}{100}\right)^{3.474}, \qquad (2)$$

The average deviation and standard deviations are 0.30% and 0.36%. The maximum deviation is found to be 0.79%. The tabulation of TC from the experiment and Eq. 2 is shown in Fig. 13. From these results, it can be seen that the experimental data are inappropriate agreement with the correlation proposed.

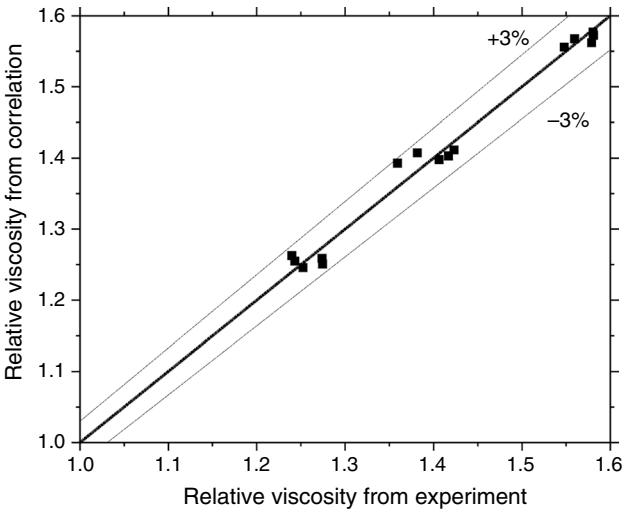

Fig. 12 Comparison between measured relative viscosity and proposed correlation

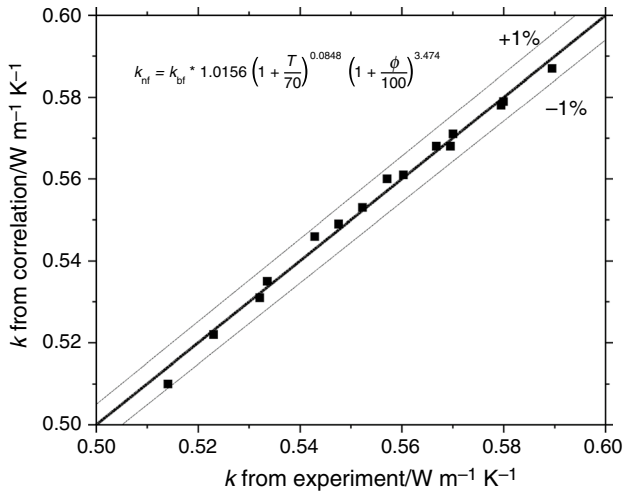

Fig. 13 Comparison between TC obtained from experiment and proposed correlation

Conclusions

Pure SiO_2, P25 nanofluids and SiO_2–P25 HNs were prepared using SiO_2 and P25 nanoparticles for characterizing the properties of nanoparticles and HNs by different techniques. The volume concentrations of nanofluid were 0.5, 1.0 and 1.5 vol%. The mixture of DI and EG at a ratio of 5:1 was used as the BF of nanofluids. The viscosity and TC of HNs were studied from 20 to 60 °C. The SEM showed that

the particle sizes of SiO_2 and P25 nanoparticles were ca. 15 nm and 10–20 nm, respectively. From XRD, the property of SiO_2 was amorphous, while P25 consisted of rutile and anatase phases. The infrared spectroscopy and elemental analysis have stated the chemical properties of nanoparticles and also the presence of functional groups on the surface of the particle. The stability of HNs was confirmed by ZP results. These nanofluids were visually observed in many days. The effective TC of HNs was improved up to 12.24% as compared to the mixture of BFs for 1.5 vol% concentration. The TC enhancement of the hybrid nanofluid was higher than the pure nanofluid. In particular, with 1.0 vol% concentration, the maximum enhancement of SiO_2, P25 and SiO_2–P25 nanofluids are 7.5%, 9.9% and 10.5%, respectively. Rheological properties were studied, and it is seen that the rheology of HNs was Newtonian behavior. The viscosity increment of SiO_2, P25 and hybrid nanofluids were 19%, 32% and 24% with 0.5 vol% concentration. Compared to the SiO_2, P25 and hybrid SiO_2–P25 nanofluids, it could be a good heat transfer fluid. The correlations of TC and viscosity for this type of nanofluid were developed. The results confirmed good accuracy.

Acknowledgements Open access funding provided by Budapest University of Technology and Economics.

Author contributions IMS and TLB were involved in conceptualization; TLB, ZIV, IEL, JM and IAB took part in methodology; ZIV and TLB carried out investigation; IMS performed funding acquisition; IMS collected the resources and supervised the study; TLB wrote the original draft; TLB, JM, SW and IMS wrote, reviewed and edited the manuscript. All authors have read and agreed to the published version of the manuscript.

Funding An NRDI K 124212 and an NRDI TNN_16 123631 Grants are acknowledged. The research within Project No. VEKOP-2.3.2-16-2017-00013 was supported by the European Union and the State of Hungary, and co-financed by the European Regional Development Fund. The research reported in this paper was supported by the Higher Education Excellence Program of the Ministry of Human Capacities in the frame of Nanotechnology and Materials Science research area of Budapest University of Technology (BME FIKP-NAT) and Stipendium Hungaricum scholarship Grant.

Compliance with ethical standards

Conflict of interest The authors declare no conflict of interest.

References

1. Masuda H, Ebata A, Teramae K. Alteration of thermal conductivity and viscosity of liquid by dispersing ultra fine particles. Netsu Bussei. 1993;7:227–33.
2. Choi SUS, Eastman JA. Enhancing thermal conductivity of fluids with nanoparticles. ASME Int Mech Eng Congr Expo. 1995;66:99–105. https://doi.org/10.1115/1.1532008.
3. Yogeswaran M, Kadirgama K, Rahman MM, Devarajan R. Temperature analysis when using ethylene-glycol-based TiO_2 as a new coolant for milling. Int J Automot Mech Eng. **ISSN** 2272–81; https://doi.org/10.15282/ijame.11.2015.10.0191.
4. Bhanvase BA, Sarode MR, Putterwar LA, Abdullah KA, Deosarkar MP, Sonawane SH. Intensification of convective heat transfer in water/ethylene glycol based nanofluids containing TiO2 nanoparticles. Chem Eng Process Process Intensif. 2014;82:123–31. https://doi.org/10.1016/j.cep.2014.06.009.
5. Mehrali M, Sadeghinezhad E, Akhiani AR, Tahan Latibari S, Talebian S, Dolatshahi-Pirouz A, Metselaar HSC, Mehrali M. An ecofriendly graphene-based nanofluid for heat transfer applications. J Clean Prod. 2016;137:555–66. https://doi.org/10.1016/j.jclepro.2016.07.136.
6. Baby TT, Ramaprabhu S. Synthesis and nanofluid application of silver nanoparticles decorated graphene. J Mater Chem. 2011;21:9702–9. https://doi.org/10.1039/c0jm04106h.
7. Ul Haq R, Khan ZH, Khan WA. Thermophysical effects of carbon nanotubes on MHD flow over a stretching surface. Phys E Low Dimens Syst Nanostruct. 2014;63:215–22. https://doi.org/10.1016/j.physe.2014.06.004.
8. Ul Haq R, Nadeem S, Khan ZH, Noor NFM. Convective heat transfer in MHD slip flow over a stretching surface in the presence of carbon nanotubes. Phys B Condens Matter. 2015;457:40–7. https://doi.org/10.1016/j.physb.2014.09.031.
9. Warrier P, Yuan Y, Beck MP, Teja AS. Heat transfer in nanoparticle suspensions: modeling the thermal conductivity of nanofluids. AIChE J. 2010;56:3243–56. https://doi.org/10.1002/aic.12228.
10. Sarkar J, Ghosh P, Adil A. A review on hybrid nanofluids: recent research, development and applications. Renew Sustain Energy Rev. 2015;43:164–77. https://doi.org/10.1016/j.rser.2014.11.023.
11. Sundar LS, Sharma KV, Singh MK, Sousa ACM. Hybrid nanofluids preparation, thermal properties, heat transfer and friction factor—a review. Renew Sustain Energy Rev. 2017;68:185–98. https://doi.org/10.1016/j.rser.2016.09.108.
12. Theres Baby T, Sundara R. Surfactant free magnetic nanofluids based on core-shell type nanoparticle decorated multiwalled carbon nanotubes. J Appl Phys. 2011. https://doi.org/10.1063/1.3642974.
13. Batmunkh M, Tanshen MR, Nine MJ, Myekhlai M, Choi H, Chung H, Jeong H. Thermal conductivity of TiO_2 nanoparticles based aqueous nanofluids with an addition of a modified silver particle. Ind Eng Chem Res. 2014;53:8445–51. https://doi.org/10.1021/ie403712f.
14. Madhesh D, Parameshwaran R, Kalaiselvam S. Experimental investigation on convective heat transfer and rheological characteristics of Cu-TiO2 hybrid nanofluids. Exp Therm Fluid Sci. 2014;52:104–15. https://doi.org/10.1016/j.expthermflusci.2013.08.026.
15. Li H, Ha C-S, Kim I. Fabrication of carbon nanotube/SiO2 and carbon nanotube/SiO2/Ag nanoparticles hybrids by using plasma treatment. Nanoscale Res Lett. 2009;4:1384–8. https://doi.org/10.1007/s11671-009-9409-4.

16. Aravind SSJ, Ramaprabhu S. Graphene-multiwalled carbon nanotube-based nanofluids for improved heat dissipation. RSC Adv. 2013;3:4199–206. https://doi.org/10.1039/c3ra22653k.
17. Le Ba T, Mahian O, Wongwises S, Szilágyi IM. Review on the recent progress in the preparation and stability of graphene-based nanofluids. J Therm Anal Calorim. 2020. https://doi.org/10.1007/s10973-020-09365-9.
18. Nabil MF, Azmi WH, Hamid KA, Zawawi NNM, Priyandoko G, Mamat R. Thermo-physical properties of hybrid nanofluids and hybrid nanolubricants: a comprehensive review on performance. Int Commun Heat Mass Transf. 2017;83:30–9. https://doi.org/10.1016/j.icheatmasstransfer.2017.03.008.
19. Ganvir RB, Walke PV, Kriplani VM. Heat transfer characteristics in nanofluid—a review. Renew Sustain Energy Rev. 2017;75:451–60. https://doi.org/10.1016/j.rser.2016.11.010.
20. Han ZH, Yang B, Kim SH, Zachariah MR. Application of hybrid sphere/carbon nanotube particles in nanofluids. Nanotechnology. 2007. https://doi.org/10.1088/0957-4484/18/10/105701.
21. Suresh S, Venkitaraj KP, Selvakumar P, Chandrasekar M. Synthesis of Al2O3-Cu/water hybrid nanofluids using two step method and its thermo physical properties. Colloids Surf A Physicochem Eng Asp. 2011;388:41–8. https://doi.org/10.1016/j.colsurfa.2011.08.005.
22. Madhesh D, Kalaiselvam S. Experimental analysis of hybrid nanofluid as a coolant. In: Procedia engineering, vol. 97. Elsevier Ltd.; 2014, pp 1667–75. https://doi.org/10.1016/j.proeng.2014.12.317.
23. Hemmat Esfe M, Abbasian Arani AA, Rezaie M, Yan WM, Karimipour A. Experimental determination of thermal conductivity and dynamic viscosity of Ag-MgO/water hybrid nanofluid. Int Commun Heat Mass Transf. 2015;66:189–95. https://doi.org/10.1016/j.icheatmasstransfer.2015.06.003.
24. Soltani O, Akbari M. Effects of temperature and particles concentration on the dynamic viscosity of MgO-MWCNT/ethylene glycol hybrid nanofluid: experimental study. Phys E Low Dimens Syst Nanostruct. 2016;84:564–70. https://doi.org/10.1016/j.physe.2016.06.015.
25. Afrand M, Toghraie D, Ruhani B. Effects of temperature and nanoparticles concentration on rheological behavior of Fe3O4-Ag/EG hybrid nanofluid: an experimental study. Exp Therm Fluid Sci. 2016;77:38–44. https://doi.org/10.1016/j.expthermflusci.2016.04.007.
26. Asadi A, Asadi M, Rezaei M, Siahmargoi M, Asadi F. The effect of temperature and solid concentration on dynamic viscosity of MWCNT/MgO (20–80)–SAE50 hybrid nano-lubricant and proposing a new correlation: an experimental study. Int Commun Heat Mass Transf. 2016;78:48–53. https://doi.org/10.1016/j.icheatmasstransfer.2016.08.021.
27. Minea AA. Hybrid nanofluids based on Al2O3, TiO2 and SiO2: numerical evaluation of different approaches. Int J Heat Mass Transf. 2017;104:852–60. https://doi.org/10.1016/j.ijheatmasstransfer.2016.09.012.
28. Bahrami M, Akbari M, Karimipour A, Afrand M. An experimental study on rheological behavior of hybrid nanofluids made of iron and copper oxide in a binary mixture of water and ethylene glycol: non-Newtonian behavior. Exp Therm Fluid Sci. 2016;79:231–7. https://doi.org/10.1016/j.expthermflusci.2016.07.015.
29. Sundar LS, Farooky MH, Sarada SN, Singh MK. Experimental thermal conductivity of ethylene glycol and water mixture based low volume concentration of Al2O3 and CuO nanofluids. Int Commun Heat Mass Transf. 2013;41:41–6. https://doi.org/10.1016/j.icheatmasstransfer.2012.11.004.
30. Zakaria I, Azmi WH, Mohamed WANW, Mamat R, Najafi G. Experimental investigation of thermal conductivity and electrical conductivity of Al2O3 nanofluid in water—ethylene glycol mixture for proton exchange membrane fuel cell application. Int Commun Heat Mass Transf. 2015;61:61–8. https://doi.org/10.1016/j.icheatmasstransfer.2014.12.015.
31. Javadi FS, Sadeghipour S, Saidur R, BoroumandJazi G, Rahmati B, Elias MM, Sohel MR. The effects of nanofluid on thermophysical properties and heat transfer characteristics of a plate heat exchanger. Int Commun Heat Mass Transf. 2013;44:58–63. https://doi.org/10.1016/j.icheatmasstransfer.2013.03.017.
32. Paul G, Philip J, Raj B, Das PK, Manna I. Synthesis, characterization, and thermal property measurement of nano-Al95Zn05 dispersed nanofluid prepared by a two-step process. Int J Heat Mass Transf. 2011;54:3783–8. https://doi.org/10.1016/j.ijheatmasstransfer.2011.02.044.
33. Azmi WH, Sharma KV, Sarma PK, Mamat R, Najafi G. Heat transfer and friction factor of water based TiO2 and SiO2 nanofluids under turbulent flow in a tube. Int Commun Heat Mass Transf. 2014;59:30–8. https://doi.org/10.1016/j.icheatmasstransfer.2014.10.007.
34. Garg J, Poudel B, Chiesa M, Gordon JB, Ma JJ, Wang JB, Ren ZF, Kang YT, Ohtani H, Nanda J, McKinley GH, Chen G. Enhanced thermal conductivity and viscosity of copper nanoparticles in ethylene glycol nanofluid. J Appl Phys. 2008;103:074301. https://doi.org/10.1063/1.2902483.
35. Nabil MF, Azmi WH, Hamid KA, Mamat R. Experimental investigation of heat transfer and friction factor of TiO2-SiO2 nanofluids in water:ethylene glycol mixture. Int J Heat Mass Transf. 2018;124:1361–9. https://doi.org/10.1016/j.ijheatmasstransfer.2018.04.143.
36. Agresti F, Barison S, Bobbo S, Colla L, Fedele L, Pagura C, Scattolini M. Thermal conductivity and viscosity measurements of water-based silica nanofluids. NSTI Nanotech. 2011;2:478–81.
37. Turgut A, Tavman I, Chirtoc M, Schuchmann HP, Sauter C, Tavman S. Thermal conductivity and viscosity measurements of water-based TiO 2 nanofluids. Int J Thermophys. 2009;30:1213–26. https://doi.org/10.1007/s10765-009-0594-2.
38. Nabil MF, Azmi WH, Abdul Hamid K, Mamat R, Hagos FY. An experimental study on the thermal conductivity and dynamic viscosity of TiO2-SiO2 nanofluids in water: ethylene glycol mixture. Int Commun Heat Mass Transf. 2017;86:181–9. https://doi.org/10.1016/j.icheatmasstransfer.2017.05.024.
39. Hamid KA, Azmi WH, Nabil MF, Mamat R. Experimental investigation of nanoparticle mixture ratios on TiO_2–SiO_2 nanofluids heat transfer performance under turbulent flow. Int J Heat Mass Transf. 2018;118:617–27. https://doi.org/10.1016/j.ijheatmasstransfer.2017.11.036.
40. Hamid KA, Azmi WH, Nabil MF, Mamat R, Sharma KV. Experimental investigation of thermal conductivity and dynamic viscosity on nanoparticle mixture ratios of TiO2-SiO2 nanofluids. Int J Heat Mass Transf. 2018;116:1143–52. https://doi.org/10.1016/j.ijheatmasstransfer.2017.09.087.
41. Evans W, Prasher R, Fish J, Meakin P, Phelan P, Keblinski P. Effect of aggregation and interfacial thermal resistance on thermal conductivity of nanocomposites and colloidal nanofluids. Int J Heat Mass Transf. 2008;51:1431–8. https://doi.org/10.1016/j.ijheatmasstransfer.2007.10.017.
42. Xuan Y, Li Q, Hu W. Aggregation structure and thermal conductivity of nanofluids. AIChE J. 2003;49:1038–43. https://doi.org/10.1002/aic.690490420.
43. Keblinski P, Eastman JA, Cahill DG. Nanofluids for thermal transport. Mater Today. 2005;8:36–44. https://doi.org/10.1016/S1369-7021(05)70936-6.
44. Sigma-Aldrich. www.sigmaaldrich.com.
45. ASHRAE. ASHRAE handbook 2001 fundamentals, vol. 53; 2001. https://doi.org/10.1017/cbo9781107415324.004.
46. Esfahani MR, Stretz HA, Wells MJM. Abiotic reversible self-assembly of fulvic and humic acid aggregates in low electrolytic conductivity solutions by dynamic light scattering and zeta

potential investigation. Sci Total Environ. 2015;537:81–92. https://doi.org/10.1016/j.scitotenv.2015.08.001.
47. Zamani L, Zomorodian K, Bi Fatemeh Mirjalili B, Khabnadideh S. One pot preparations 1-amidoalkyl-2-naphthols derivative catalyzed by nano-TiCl4.SiO2 with antimicrobial studies of some products. J Pharm Sci Innov. 2014;3:208–16. https://doi.org/10.7897/2277-4572.033141.
48. Theivasanthi T, Alagar M. Titanium dioxide (TiO_2) nanoparticles-XRD analyses—an insight. arXiv preprint 2013. arXiv:1307.1091
49. Thangavelu K, Annamalai R, Arulnandhi D. Preparation and characterization of nanosized TiO_2 powder by sol-gel precipitation route. Int J Emerg Technol Adv Eng. 2013;3:636–9.
50. Yu W, Xie H. A review on nanofluids: preparation, stability mechanisms, and applications. J Nanomater. 2011. https://doi.org/10.1155/2012/435873.
51. Le Ba T, Mahian O, Wongwises S, Szilágyi IM. Review on the recent progress in the preparation and stability of graphene-based nanofluids. J Therm Anal Calorim. 2020. https://doi.org/10.1007/s10973-020-09365-9.
52. Nguyen CT, Desgranges F, Roy G, Galanis N, Maré T, Boucher S, Angue Mintsa H. Temperature and particle-size dependent viscosity data for water-based nanofluids—hysteresis phenomenon. Int J Heat Fluid Flow. 2007;28:1492–506. https://doi.org/10.1016/j.ijheatfluidflow.2007.02.004.
53. Chen H, Ding Y. Heat transfer and rheological behaviour of nanofluids—a review. Berlin: Springer; 2009. p. 135–77. https://doi.org/10.1007/978-3-642-02690-4_3.
54. Mehrali M, Sadeghinezhad E, Latibari S, Kazi S, Mehrali M, Zubir MNBM, Metselaar HS. Investigation of thermal conductivity and rheological properties of nanofluids containing graphene nanoplatelets. Nanoscale Res Lett. 2014;9:15. https://doi.org/10.1186/1556-276x-9-15.
55. Jang SP, Choi SUS. Role of Brownian motion in the enhanced thermal conductivity of nanofluids. Appl Phys Lett. 2004;84:4316–8. https://doi.org/10.1063/1.1756684.